Algorithms for On-Board Orbit Determination using GPS OBODE-GPS

Technical Report · January 2000

Source: DLR

ana paula marins Chiaradia
São Paulo State University

Eberhard Gill
Delft University of Technology

Helio Koiti Kuga
National Institute for Space Research, Brazil

DLR – GSOC TN 00-04

Algorithms for On-Board Orbit Determination using GPS
OBODE-GPS

Chiaradia A.P.M.; Gill E.; Montenbruck O.;
Kuga H.K.; Prado A.F.B.A.
2000

DLR
German Space Operations Center
Oberpfaffenhofen

CONTENTS

1. INTRODUCTION

This report describes the results of a project developed under the cooperation program between the Brazilian Space Research Institute (INPE) and the German Space Operations Center (GSOC) of the German Aerospace Center (DLR). The work has been performed in the field of precise satellite orbit determination using Global Positioning System (GPS) and Kalman Filter.

This project consists of developing a software to onboard orbit determination in real time using the GPS (OBODE-GPS), and analyzing some relevant issues about the orbit determination. The main goal of the OBODE-GPS is to have a relatively standard accuracy (around tens of meters) along with minimum computational cost and usage of a simplified model. For this sake, only the GPS code pseudorange in L1 frequency is used considering the effects of the clock offsets of the GPS and user satellites, and user relativistic effects. Also, a dynamic model with geopotential effect is considered; where to propagate the state covariance matrix, it is considered a simpler model than the one used in the dynamical model. The Cowell's method is used to propagate the orbit state vector; and a simple 4^{th} order Runge-Kutta (RK4) algorithm is used without any mechanism of step adjustment or error control. The conventional extended Kalman Filter is used to estimate in real time the spacecraft's orbit onboard. To validate this model, real data from Topex/Poseidon satellite, which has a dual frequency GPS receiver onboard, are used, and the results are compared with the Topex/Poseidon Precision Orbit Ephemeris (POE) generated by NASA/JPL.

The following points have been analyzed:

As regards the dynamic model:

- A study about the order and degree truncation of the spherical harmonic coefficients of the JGM-2 model considering low computational cost, relative accuracy (tens of meters), and the lowest possible order and degree.
- A study about the step size of the RK4 integrator considering low computational cost, relative accuracy, and the largest possible step size.
- The selection of appropriate reference systems and transformations.

As regards the filtering:

- The standard Kalman filtering is used.
- A study about the use of the simplified transition matrix considering either the pure Keplerian motion or including the J_2 effects.

As regards the GPS:

- Comparison of the GPS broadcast ephemeris with the GPS precise ephemeris (SP3 format).

In Chapter 2, the coordinate and time systems used in the software OBODE-GPS are presented. The ToD (True of Date) and UTC time are the coordinate and time systems used throughout the software. The only coordinate transformation considered is the rotation from the Earth-fixed frame to the inertial ToD frame through the sidereal time. As regards the time transformation, UTC to GPS time was taken into account.

In Chapter 3, the force model is presented. The only force acting on an artificial satellite considered was due to Earth's gravitacional field implemented according to Pines (1973) and the gravitational model coefficients considered were the JGM-2 (Tapley, 1994).

In Chapter 4, the algorithm of the simple 4^{th} order Runge-Kutta (RK4) is presented.

In Chapter 5, the pseudorange measurement model is presented. The clock term error and the GPS travel and reception time correction are also presented as implemented in the software.

In Chapter 6, the algorithm of the extended Kalman filter and how it has been applied for orbit determination is presented.

In Chapter 7, two methods for propagating the transition matrix are presented. One of them considers only the Keplerian motion and the other considers the effects of J_2.

In Chapter 8, the data set is described. A brief description of the Topex/Poseidon is done.

In Chapter 9, the broadcast ephemerides analyses are presented. Some results are also presented.

In Chapter 10, the studies about the order and degree truncation of the spherical harmonic coefficients of the JGM-2 model, the step size of the RK4 integrator, and the use of the simplified transition matrix considering only the Keplerian motion or $J_{2,}$ are presented. The initial conditions used throughout the tests are also presented.

In Chapter 11, the conclusions of this work are presented.

In Chapter 12, the references cited in this work can be found.

2. COORDINATE AND TIME SYSTEMS

This present chapter describes the coordinate and time transformations used in the software OBODE-GPS. The adopted coordinate and time systems for the whole software is ToD (True of Date) in UTC (Universal Coordinated Time) time. However, other systems are adopted in some routines requiring specific transformations during the estimation process.

As regards the coordinate transformation, the True-of-Date system is used for the integration of the equations of motion within OBODE-GPS. However, for computing the acceleration of the satellite due to geopotential, the coordinates of the satellite shall be in Earth-fixed system. Therefore, it is necessary to make a transformation from ToD to EF and vice versa.

The input and output of GPS broadcast data are in Earth-fixed WGS-84 system and in GPS time. Then, the GPS positions are calculated using the broadcast message in that system. For computing the pseudorange, the coordinates of the receiver and the GPS shall be in the same system. Then it is necessary to make a transformation in the coordinates of the receiver from ToD to EF (Earth-fixed equator and prime meridian), which considers the effect of polar motion. However, the effect of polar motion is neglected in this software, because it is small as well as to save computational burden. Therefore, the considered transformation is from ToD to PEF (Pseudo-Earth-fixed equator and prime meridian), which considers primarily the sidereal rotation.

As regards the time transformation, the navigation message and the observations are broadcast in GPS time. Therefore, it is necessary to make a transformation from GPS time to UTC time.

Next, these transformations are shown in a summarized way. For more details, see (Kuga and Gill, 1994) and (Hofmann-Wellenhof *et. al.*, 1994).

2.1 Coordinate System Transformation

The transformation from ToD to PEF coordinates takes into account the rotation of the Greenwich prime meridian with respect to the true of date inertial system. Therefore this transformation relates the true of date inertial coordinates to the geographical coordinates corresponding to the rotating Earth (Montenbruck & Gill 2000).

Transformations from ToD to PEF – The Sidereal Rotation

The transformation from ToD to PEF is given by:

$$\boldsymbol{r}_{PEF} = \boldsymbol{R}_{\theta}\boldsymbol{r}_{ToD} \tag{2.1}$$

with the sidereal rotation matrix $\boldsymbol{R}_{\boldsymbol{\theta}}$ given by:

$$\boldsymbol{R}_{\theta} = \begin{pmatrix} +\cos\theta & +\sin\theta & 0 \\ -\sin\theta & +\cos\theta & 0 \\ 0 & 0 & 1 \end{pmatrix} \tag{2.2}$$

where θ denotes the so-called Greenwich true (or apparent) sidereal time of the date. It is computed taking into account the equation of equinoxes and the time UT1 (Universal Time corrected for polar motion). In this software, it is calculated in UTC time, as will be shown.

The true Greenwich sidereal time can be computed by:

$$\theta = 1.0027379093\tau_{UT1} + \bar{\theta}_0 + \Delta\varphi\cos\varepsilon' \tag{2.3}$$

where the first term on the right side accounts for the different scales of solar and sidereal time, $\Delta\varphi\cos\varepsilon'$ is known as equation of equinoxes, being a function of the nutation in longitude $\Delta\varphi$ and the true obliquity of the ecliptic ε', and

$$\bar{\theta}_0 = 24110.54841 + 8640184.812866T + 0.093104T^2 - 6.2\times10^{-6}T^3 \tag{2.4}$$

where $\bar{\theta}_0$, in seconds, is the Greenwich mean sidereal time at 0^h UT1 of the day, T is the number of Julian centuries since J2000.0 to 0^h UT1 of the date. In this software, this equation is considered constant during the whole day.

The velocity components of the state vector are obtained through their dependence on the sidereal time:

$$\dot{\boldsymbol{r}}_{PEF} = \boldsymbol{R}_{\theta}\dot{r}_{ToD} + \dot{\boldsymbol{R}}_{\theta}\boldsymbol{r}_{ToD} \tag{2.5}$$

with the time rate $\dot{\boldsymbol{R}}_{\theta}$ of the sidereal rotation matrix expressed as:

$$\dot{\boldsymbol{R}}_{\theta}\boldsymbol{r}_{ToD} = \boldsymbol{R}_{\theta}(\omega\times\boldsymbol{r}_{ToD}) \tag{2.6}$$

and the sidereal rotation rate vector $\omega^T = (0,0,\dot{\theta})$. Then,

$$\dot{\boldsymbol{R}}_\theta = \dot{\theta}\begin{bmatrix} -\sin\theta & +\cos\theta & 0 \\ -\cos\theta & -\sin\theta & 0 \\ 0 & 0 & 0 \end{bmatrix}. \tag{2.7}$$

The inverse transformation is achieved by:

$$\boldsymbol{r}_{ToD} = \boldsymbol{R}_\theta^T \boldsymbol{r}_{PEF} \tag{2.8}$$

and

$$\dot{\boldsymbol{r}}_{ToD} = \boldsymbol{R}_\theta^T \dot{\boldsymbol{r}}_{PEF} + \dot{\boldsymbol{R}}_\theta^T \boldsymbol{r}_{PEF}\,. \tag{2.9}$$

The used constants of WGS-84 model are shown in Table 2.1.

Table 2.1: Constants of the WGS-84 model

Earth's radius	6378137.0 m
Flattening factor	1./298.257223563
Earth's gravitational coefficient	3.986005×10^{14} m^3/s^2
Earth's rotation rate	$7.2921151467\times10^{-5}$ rad/s

2.2 Time Transformation

Universal Time (UT) and sidereal time are based on the Earth's rotation. Universal Time is defined by the Greenwich hour angle augmented by 12 hours of a fictitious sun uniformly orbiting in the equatorial plane. Sidereal time is defined by the hour angle of the vernal equinox. UT1 is the universal time of the Greenwich Meridian and it measures the true angular rotation of the Earth as corrected for the rotational component induced by polar motion. However, in practice, the dynamic time system is achieved by the use of atomic time scales which is not related to the Earth's rotation. Atomic time is tied to the Earth's rotation by the introduction of the Universal Coordinated Time (UTC) time scale. The time UT1 is related to UTC by the quantity dUT1, which is time dependent and it is reported by the International Earth Rotation Service (IERS):

$$UT1 = UTC + dUT1\,. \tag{2.10}$$

When $|UT1 - UTC|$ becomes larger than 0.9 s, a leap second is inserted into the UTC system (Hofmann-Wellenhof *et. al.*, 1994). In this software, the UTC is considered equal to UT1.

GPS Time is the time scale adopted in the broadcast ephemeris and it is related to the atomic time system. The conversion between the UTC and GPS times is achieved by the formula:

$$UTC + 1.000\eta = GPS + 19.000 \text{ [s]} \tag{2.11}$$

where η is the actual integer reported by the IERS. The GPS time was coincident with UTC at the GPS standard epoch 1980, January 6th (Hofmann-Wellenhof *et. al*., 1994).

3. FORCE MODEL

This present chapter describes the modeling of the forces and its partial derivatives used in the OBODE-GPS. Based on this modeling, the equations of motion and the variational equations are numerically integrated over the time interval as shown in the next chapter.

The main forces acting on an artificial satellite may be classified as gravitational force (geopotential, third-body perturbations) and non-gravitational forces (atmospheric drag, solar radiation pressure). The most important force acting on a low altitude satellite (below 1000 km) is due to the central body gravity field and the atmospheric drag. In a high altitude (above 1000 km) the most important forces are due to the third-body perturbation and to the solar radiation pressure. Above 1000 km, the solar radiation pressure is usually stronger than atmospheric drag (Kuga, 1982).

These forces are difficult to be modeled and a mathematically inaccurate model of the motion with respect to true motion is sometimes adopted, which can become critical for the orbit determination. In principle, a simplified model can be adopted to save processing time, mainly in real time processing.

Therefore only forces due to the Earth's gravitational field up to order and degree 50 were considered.

3.1 Geopotential

The spacecraft acceleration vector $\boldsymbol{a}_{GEO}$ due to the geopotential is given by:

$$\boldsymbol{a}_{GEO} = \frac{\partial \boldsymbol{U}}{\partial \boldsymbol{r}} \tag{3.1}$$

where $\boldsymbol{r}$ is the inertial position vector and $\boldsymbol{U}$ is the gravity potential of the Earth. The corresponding partial derivatives matrix to be used in the variational equations is given by $\partial \boldsymbol{a}_{GEO} / \partial \boldsymbol{r}$.

The representation of the gravity field is usually done using spherical harmonics:

$$\boldsymbol{U}(r,\phi,\lambda) = \frac{\mu}{r}\sum_{n=0}^{\infty}\sum_{m=0}^{n}\left(\frac{r_e}{r}\right)^n \overline{P}_{n,m}(sin\phi)\left[\overline{C}_{n,m}\cos m\lambda + \overline{S}_{n,m} sin m\lambda\right] \tag{3.2}$$

where μ is the central body's gravitational coefficient, r_e is the radius of the central body, r is the satellite radial distance, ϕ is the geocentric latitude, and λ is the longitude in Earth fixed coordinates. The values $\overline{C}_{n,m}$ and $\overline{S}_{n,m}$ are the normalized spherical harmonic coefficients of degree *n* and order *m*, while $\overline{P}_{n,m}$ are the normalized associated Legrende functions of degree *n* and order *m.* The constants μ, r_e, $\overline{C}_{n,m}$, and $\overline{S}_{n,m}$ are the coefficients that define a specific gravity potential. The associated Legendre functions can be found by evaluating:

$$P_{n,m}(\sin\phi) = \frac{1}{2^n\, n!} \frac{d^{n*m}}{d \sin\phi^{n+m}} \left(\sin^2\phi - 1\right)^n . \tag{3.3}$$

The dynamic equation of motion is then given by:

$$\ddot{r} = a_{\boldsymbol{GEO}} . \tag{3.4}$$

The acceleration and the partial derivatives matrix are computed through the recurrence relations according to Pines (1973) in Earth-fixed coordinates. In the present implementation, the JGM-2 complete to order and degree 50 is available (Tapley, 1994). In Table 3.1, some of the JGM-2 constants are shown.

Table 3.1: Constants of the JGM-2 model

Earth's radius	6378136.3 m
Earth's gravitational coefficient	3.986004415×10^{14} m^3/s^2
2nd zonal coefficient	$-.10826269\times10^{-2}$

4. NUMERICAL INTEGRATION

The orbit propagation method is one of the most important problems in analyzing and controlling missions which involves artificial satellites. In practice, the numerical method is the most used one, as the Cowell's method. The Cowell's method consists of integrating the satellite's equations of motion with all perturbations step by step and it involves straight integration of velocity and acceleration time step. The perturbations can be included in the same time. The acceleration is found by evaluating the forces acting on the spacecraft.

The integration is carried out by using the simple 4th order Runge-Kutta (RK4) algorithm without any mechanism of step adjustment or error control. The RK4 is considered an adequate numerical integrator due to its simplicity, fair accuracy, low truncation error, and low computational burden. It does not need an initialization procedure and the step size is easy to change. The RK4 algorithm is as follows:

$$y_{k+1} = y_j + \Delta t\left[\frac{1}{6} f\left(y_k, t_k\right) + \frac{1}{3} f\left(y^*_{k+1/2}, t_{k+1/2}\right) + \frac{1}{3} f\left(y^{**}_{k+1/2}, t_{k+1/2}\right) + \frac{1}{6} f\left(y^*_{k+1}, t_{k+1}\right)\right] \tag{4.1}$$

where

$$\begin{aligned} y^*_{k+1/2} &= y_k + \frac{\Delta t}{2} f\left(y_k, t_k\right), \\ y^{**}_{k+1/2} &= y_k + \frac{\Delta t}{2} f\left(y^*_{k+1/2}, t_{k+1/2}\right), \\ y^*_{k+1} &= y_k + \Delta t f\left(y^{**}_{k+1/2}, t_{k+1/2}\right). \end{aligned} \tag{4.2}$$

It is initialized by specifying the initial spacecraft state y_k at some epoch t_k. It continues by specifying an integration time step, Δt, and evaluating Equations 4.2 in the order presented here and then substituting those equations into Equation 4.1. The variable $f\left(y_k, t_k\right)$ represents the derivatives of the spacecraft state vector, i.e. velocity and acceleration, on the spacecraft at time t_k and state y_k. For more information and details about numerical integrators, see (Kondapalli, 1984).

5. MEASUREMENT MODEL

The GPS provides two kinds of measurements, the code and carrier phase pseudoranges, besides the navigation solution. Pseudorange is the range between the phase centers of the GPS satellite and the receiver antennas, plus the offset between the transmitter and receiver clocks. The pseudorange measurements, however, are corrupted by various error sources. The error sources can steam from three groups: satellite (clock bias and orbital errors), signal propagation (ionospheric and tropospheric refraction), and receiver (antenna phase center variation, clock bias, and multipath).

For high-precision applications, the use of the raw code and carrier phase measurements is required. The code pseudorange or GPS navigation solution can be used to determine the orbit providing the accuracy required by the mission as in this work.

5.1 Code Pseudorange Measurement

The considered errors in the code pseudorange measurements were the GPS satellite and receiver clock bias. Therefore, the equation of the code pseudorange in L1 frequency is given by:

$$y_c = \rho + c[\Delta t_{sv}(t) - \Delta t_u(t)], \tag{5.1}$$

where y_c is the code pseudorange on L1, c is the vacuum speed of light, $\Delta t_{sv}(t)$ is the GPS satellite clock offset, $\Delta t_u(t)$ is the receiver clock offset, t is the observation instant in GPS time, ρ is the range given by:

$$\rho = \sqrt{(x_{GPS} - x)^2 + (y_{GPS} - y)^2 + (z_{GPS} - z)^2}\ , \tag{5.2}$$

where x, y, and z are the positional states of the user satellite at the reception time and x_{GPS}, y_{GPS}, and z_{GPS} in WGS-84 are the positional states of the GPS satellite at the transmission time (corrected for light time delay).

Clock term error

The second term of the right-side of the Equation 5.1 is the clock bias that represents the combined clock offsets of the satellite and of the receiver with respect to the GPS time. Each GPS satellite contributes with one clock bias. The information for the GPS satellite clocks is known and transmitted via the broadcast navigation message in the form of three polynomial coefficients with a reference time t_{oc}. The clock correction of the GPS satellite for the epoch t is:

$$t = t_{sv} - \Delta t_{sv} \tag{5.3}$$

where

$$\Delta t_{SV} = a_{f0} + a_{f1}(t - t_{oc}) + a_{f2}(t - t_{oc})^2 + \delta_R^{GPS}, \tag{5.4}$$

and

$$\delta_R = \frac{2}{c^2}\sqrt{a\mu} e sin E, \tag{5.5}$$

where t_{sv} is the spacecraft code phase time at the message transmission time in seconds; t_{oc} is the reference time, in seconds, measured from the GPS time weekly epoch; a_{f0}, a_{f1}, and a_{f2} are parameters; δ_R is a small relativistic clock correction caused by the orbital eccentricity e; a is the semi-major axis of the orbit; and E is the eccentric anomaly. Relativistic effects are relevant for the satellite orbit, the satellite signal propagation, and both the GPS satellite and receiver clock, but it can be accurately computed. For GPS orbits with eccentricity 0.02 this effect can be as large as 45.8 ns, corresponding to a ranging error of about 14 m (Leick, 1994). The relativistic effect is included in the clock polynomial broadcast via the navigation message, where the time dependent eccentric anomaly E is expanded into a Taylor series. If a more accurate equation is required, the relativistic effects must be subtracted from the clock polynomial coefficients. The polynomial coefficients a_{f0}, a_{f1}, and a_{f2} are transmitted in units of sec, sec/sec, and sec/sec^2, respectively. The clock data reference time t_{oc} is also broadcast. The value of t_{sv} must account for the beginning or the end-of-week crossovers. The user may approximate t by t_{sv} in Equation 5.3. The user clock offset is part of the estimated state vector given by:

$$c\Delta t_u = b + \dot{b}\Delta t + \ddot{b}\Delta t^2 + \delta_R^{USER} \tag{5.6}$$

where b is the receiver clock bias, $\dot{b}$ is the drift, $\ddot{b}$ is half the drift rate and Δt is the elapsed time of measurements. The relativistic effect in the user clock is calculated by using the best available estimated state vector in the epoch.

5.2 GPS Travel and Reception Time

Computation of the geometric range, ρ, is required for both pseudorange and carrier phase processing. The GPS position coordinates are used at the instant of emission. However, the reception time is used to compute it. Then, it is necessary to correct this time by subtracting the travel time of signal to obtain the emission time. Therefore it is necessary to compute the travel time through an iterative process that starts assuming an average value for the travel time τ. Next, it is interpolated the GPS position for the epoch (t - τ) and, then, geometric range is computed, which is used to recompute the travel time by:

$$\tau = \frac{\rho}{c}\,. \tag{5.7}$$

The light-time iteration is usually performed in an inertial system with position vector $\boldsymbol{x} = (x, y, z)$ and the GPS satellite position vector $\boldsymbol{x_{GPS}} = (x_{GPS}, y_{GPS}, z_{GPS})$. Then, it is necessary to transform the positions from inertial to the Earth-fixed WGS84 system. So, the signal path is given by Montenbruck & Gill (2000):

$$\rho = \boldsymbol{R}_{WGS}(t)\left(\boldsymbol{x}_{GPS}(t-\tau) - \boldsymbol{x}(t)\right) \tag{5.8}$$

where $\boldsymbol{R}_{WGS}(t)$ is the rotation matrix from inertial to Earth-fixed WGS-84 system. Making use of the approximation

$$\boldsymbol{R}_{WGS}(t) \approx \boldsymbol{R}_z(\omega_e\tau)\boldsymbol{R}_{WGS}(t-\tau) \tag{5.9}$$

where ω_e is the Earth's rotation rate, the inertial position of the GPS satellite may be substituted by the corresponding Earth-fixed position:

$$\boldsymbol{x}_{GPS}^{WGS}(t-\tau) = \boldsymbol{R}_{WGS}(t-\tau)\boldsymbol{x}_{GPS}(t-\tau)\,. \tag{5.10}$$

This yields

$$\rho = c\tau = \left|\boldsymbol{R}_z(\omega_e\tau)\boldsymbol{x}_{GPS}(t-\tau) - \boldsymbol{x}^{WGS}(t)\right| \tag{5.11}$$

in the Earth-fixed reference frame.

If the discrepancy between the first and second approximation of τ is greater than a specified criterion, the iteration is repeated, i.e., a new satellite position is interpolated and a new distance is computed, and so on. Generally, a couple of iterations are sufficient.

This computation is not affected by the receiver clock error $\Delta t_u(t)$ and the satellite clock error $\Delta t_{sv}(t)$. However, the computed nominal emission time is corrupted by the ionospheric, tropospheric, hardware, and multipath. All of these effects are negligible in the present context. The reception time is corrected by the same process, too.

6. ESTIMATION TECHNIQUE

The orbit determination problem, which has a non-linear dynamical system and a non-linear measurement system, can be formulated in a way that makes it possible to apply one of the best known methods of sequential linear estimation, the Kalman filter.

The Kalman filter is used to estimate the spacecraft's orbit onboard because it excludes the requirement of iterating the data collected previously and it is able to provide the current orbit in real time.

The orbit determination process consists of obtaining values of the parameters which completely specify the motion of an orbiting body, like satellite through space, based on a set of observations of the body.

Let

$$\dot{\boldsymbol{x}}(t) = \boldsymbol{f}(\boldsymbol{x},t) + \boldsymbol{w}(t) \tag{6.1}$$

be a non-linear dynamical system, where $\boldsymbol{x}$ is the state vector to be estimated, $\boldsymbol{f}(\boldsymbol{x},t)$ is the vector-valued function of the time and the state, and $\boldsymbol{w}$ an uncorrelated Gaussian noise sequence of the state with a zero Gaussian mean and white sequence with covariance $\boldsymbol{Q}_k$. ($\boldsymbol{w}$ ~ $N_k(0, Q_k)$); and let

$$\boldsymbol{y}_k = \boldsymbol{h}_k(\boldsymbol{x}_k, t) + \boldsymbol{v}_k \tag{6.2}$$

be a discrete non-linear measurement model, where $\boldsymbol{y}$ is the measurement vector, $\boldsymbol{h}$ is the vector function of state and time, and $\boldsymbol{v}$ is an uncorrelated Gaussian noise sequence of measurement with a zero mean and white sequence with covariance $\boldsymbol{R_k}$, that is, $\boldsymbol{v}$ ~ $N_k(0, R_k)$. For more details and information about estimation techniques, see Gelb (1974) and Maybeck (1979).

6.1 Extended Kalman Filter

The extended Kalman filter is a version applicable to non-linear problems and is composed by a time-update and a measurement-update cycles. The time-update phase updates the state and the covariance matrix along the time using the dynamical equations.

The differential dynamic equations of motion to be integrated are given by:

$$\dot{\boldsymbol{x}} = \boldsymbol{f}(\boldsymbol{x},t) \tag{6.3}$$

where $\boldsymbol{f}(\boldsymbol{x},t)$ is the vector-valued function of time and the state and the estimated state vector is given by:

$$\boldsymbol{x} = \left(\boldsymbol{r},\boldsymbol{v},b,\dot{b},\ddot{b}\right)^T , \tag{6.4}$$

where $\boldsymbol{r} = (x, y, z)^T$ and $\boldsymbol{v} = (\dot{x}, \dot{y}, \dot{z})^T$ are the spacecraft's position and velocity vector, b is the receiver clock bias, $\dot{b}$ is the drift, $\ddot{b}$ is half the drift rate, and t is the instant of integration. The position coordinates are in meter unit, velocity coordinates in meter/second unit. All coordinates refer to the ToD system.

The solution of the equation of motion for an adopted force model and given initial conditions of the state vector at epoch t can be supplemented by the solution of the associated variational equations:

$$\dot{\boldsymbol{\Phi}} = \boldsymbol{F}\boldsymbol{\Phi} \tag{6.5}$$

where $\boldsymbol{\Phi}$ is the state transition matrix which relates the state deviation between t_k and t_{k+1}, and $\boldsymbol{F} = \partial \boldsymbol{f}(\boldsymbol{x},t)/\partial \boldsymbol{x}$. The equations of motion are integrated considering perturbations due to the geopotential as shown in Chapter 3 and integrated by RK4 as shown in Chapter 4. The integration of the transition matrix will be shown in Chapter 7.

Both equations should be integrated simultaneously, so that $\boldsymbol{F}$ is evaluated always along the most current state $\boldsymbol{x}$. Next, one updates the covariance matrix $\boldsymbol{P}$ by means of the discrete Riccatti equation:

$$\overline{\boldsymbol{P}}_{k+1} = \boldsymbol{\Phi}_{k+1}\hat{\boldsymbol{P}}_k\boldsymbol{\Phi}^T_{k+1} + \boldsymbol{Q}_k , \tag{6.6}$$

where $\hat{\boldsymbol{P}}_k$ is the covariance matrix after processing all measurements at time t_k, $\boldsymbol{\Phi}$ is the state transition matrix obtained by the previous integration and $\boldsymbol{Q}_k$ is the discrete state-noise covariance, which is a measurement of the error between the reference state and the true state arising from imperfect modeling. The $\boldsymbol{P}_k$ matrix is a measurement of accuracy of the errors.

At the end of this process, $\overline{\boldsymbol{x}}_{k+1}$ and $\overline{\boldsymbol{P}}_{k+1}$, are obtained and are called time-updated state and covariance, respectively.

The measurement residual and the sensitivity matrix are found by forming the computed observation equation. The model for the GPS pseudorange measurement is given by the Equation 5.1.

Using the code pseudorange, the sensitivity matrix will be given by:

$$\boldsymbol{H}_k = \left[-\frac{(x_{GPS} - x)}{\rho} \quad -\frac{(y_{GPS} - y)}{\rho} \quad -\frac{(z_{GPS} - z)}{\rho} \quad 0 \quad 0 \quad 0 \quad 1 \quad \Delta t \quad \Delta t^2 \right], \tag{6.7}$$

where Δt is the elapsed time of measurements.

The measurement residual is:

$$\boldsymbol{y}_k = \boldsymbol{Y}_k - \boldsymbol{y}_c(\, \boldsymbol{x}_k, t_k \,), \tag{6.8}$$

where $\boldsymbol{Y}_k$ is the observed measurement and $\boldsymbol{y}_c$ is the calculated measurement by the Equation 5.1.

The measurement update phase uses the Kalman equations to incorporate the information given by the measurements themselves, and obtains improved estimates of the state and of the covariance:

$$\boldsymbol{K}_k = \overline{\boldsymbol{P}}_k \boldsymbol{H}_k^T \left(\boldsymbol{H}_k \overline{\boldsymbol{P}}_k \boldsymbol{H}_k^T + \boldsymbol{R}_k \right)^{-1}, \tag{6.9}$$

$$\hat{\boldsymbol{x}}_k = \overline{\boldsymbol{x}}_k + \boldsymbol{K}_k \boldsymbol{y}_k, \tag{6.10}$$

$$\hat{\boldsymbol{P}}_k = \left(\boldsymbol{I} - \boldsymbol{K}_k \boldsymbol{H}_k \right) \overline{\boldsymbol{P}}_k, \tag{6.11}$$

where $\boldsymbol{R_k}$ is the discrete measurement noise covariance, which is basically a measurement weight matrix. These equations can be used to process the measurements sequentially so that the matrix inversion in Equation 6.9 is of a scalar. To be precise, the measurements should be uncorrelated, in which case the measurement covariance noise $\boldsymbol{R}_{\mathrm{k}}$ is diagonal.

7. TRANSITION MATRIX

The function of the transition matrix is to relate the rectangular coordinate variations between the times t_k and t_{k+1}. Also, it can be used to relate the residuals between the observed and calculated measurements in the orbit determination. The more precise the transition matrix, the better the orbit determination.

However, the evaluation of the state transition matrix presents one of the highest computational costs because it requires the evaluation of the Jacobian matrix (partial derivatives) and the integration of the current variational equations. This matrix can pose cumbersome analytical expressions when using a complex force model.

One method to avoid the problem of the high computational cost and the extended analytical expressions of the transition matrix consists of propagating the state vector using the complete force model and, then, to compute the transition matrix using a simplified force model. The adopted force model for the transition matrix considers only the Keplerian motion, which is a reasonable approximation when only short time intervals between the observations and reference instant are involved (Kuga, 1986). The other alternative implementation for transition matrix is to consider the J_2 effect according to the Markley's method (1986). These two implementations are done to check if there is some improvement or degradation in the estimated state. The results are shown in the Chapter 10.

Goodyear (1965) published a method for the analytical calculation of a transition matrix for the two-body problem. This method is valid for any kind of orbit. Kuga (1986) has implemented this method using the same elegant and adequate formulation to digital implementation, but applied to the Keplerian elliptical orbit problem. He has done possible simplifications in this method to increase its numerical efficiency (processing time, memory, and precision).

The Markley's method uses two states, one in t_{k-1} time and other in t_k time, and calculates the transition matrix between them by using μ, J_2, Δt, the radius of the Earth, and the two states. In this case, the effect of the Earth's flattening is the most influent factor in the process. The Markley's method consists of making one approximation to the transition matrix of the state vector based on Taylor series expansion for short intervals of propagation, Δt. This method will be shown in 7.2 (Markley, 1986).

7.1 First Method: The Analytical Transition Matrix Solution for the Keplerian Elliptical Orbit

The differential equation for the Keplerian motion is expressed by:

$$\ddot{\boldsymbol{r}} = -\frac{\mu \boldsymbol{r}}{r^3}, \tag{7.1}$$

where

$$r = \sqrt{x^2 + y^2 + z^2}\ . \tag{7.2}$$

The equation that relates the state deviations in different times is given by:

$$\begin{pmatrix} \delta r \\ \delta v \end{pmatrix} = \Phi(\boldsymbol{t}, \boldsymbol{t}_0) \begin{pmatrix} \delta r_0 \\ \delta v_0 \end{pmatrix}, \tag{7.3}$$

where $\boldsymbol{r}$ and $\boldsymbol{v}$ are the position and velocity coordinates in the time t, respectively; $\boldsymbol{r_0}$ and $\boldsymbol{v_0}$ are the initial position and velocity coordinates in the time t_0, respectively; and $\boldsymbol{\Phi}$ is the transition matrix given by:

$$\boldsymbol{\Phi} = \begin{pmatrix} \boldsymbol{\Phi}_{11} & \boldsymbol{\Phi}_{12} \\ \boldsymbol{\Phi}_{21} & \boldsymbol{\Phi}_{22} \end{pmatrix} = \begin{pmatrix} \dfrac{\partial \boldsymbol{r}}{\partial \boldsymbol{r}_0} & \dfrac{\partial \boldsymbol{r}}{\partial \boldsymbol{v}_0} \\ \dfrac{\partial \boldsymbol{v}}{\partial \boldsymbol{r}_0} & \dfrac{\partial \boldsymbol{v}}{\partial \boldsymbol{v}_0} \end{pmatrix}. \tag{7.4}$$

According to Goodyear (1965, 1966) and Shepperd (1985), the four submatrices 3x3 are written as:

$$\begin{aligned}
\boldsymbol{\Phi}_{11} &= f\boldsymbol{I} + \begin{pmatrix} \boldsymbol{r} \\ \boldsymbol{v} \end{pmatrix} \begin{pmatrix} M_{21} & M_{22} \\ M_{31} & M_{32} \end{pmatrix} \begin{pmatrix} \boldsymbol{r}_0 \\ \boldsymbol{v}_0 \end{pmatrix}^T, \\
\boldsymbol{\Phi}_{12} &= g\boldsymbol{I} + \begin{pmatrix} \boldsymbol{r} \\ \boldsymbol{v} \end{pmatrix} \begin{pmatrix} M_{22} & M_{23} \\ M_{32} & M_{33} \end{pmatrix} \begin{pmatrix} \boldsymbol{r}_0 \\ \boldsymbol{v}_0 \end{pmatrix}^T, \\
\boldsymbol{\Phi}_{21} &= \dot{f}\boldsymbol{I} - \begin{pmatrix} \boldsymbol{r} \\ \boldsymbol{v} \end{pmatrix} \begin{pmatrix} M_{11} & M_{12} \\ M_{21} & M_{22} \end{pmatrix} \begin{pmatrix} \boldsymbol{r}_0 \\ \boldsymbol{v}_0 \end{pmatrix}^T, \\
\boldsymbol{\Phi}_{22} &= \dot{g}\boldsymbol{I} - \begin{pmatrix} \boldsymbol{r} \\ \boldsymbol{v} \end{pmatrix} \begin{pmatrix} M_{12} & M_{13} \\ M_{22} & M_{23} \end{pmatrix} \begin{pmatrix} \boldsymbol{r}_0 \\ \boldsymbol{v}_0 \end{pmatrix}^T,
\end{aligned} \tag{7.5}$$

where $\boldsymbol{I}$ is the identity matrix 3x3; the $\boldsymbol{M}_{i,j}$, i, j = 1,2,3 are the components of a matrix $\boldsymbol{M}_{3x3}$ which will be shown later, and f, g, $\dot{f}$, $\dot{g}$ are calculated in the next topic.

Calculating the functions f, g, $\dot{f}, \dot{g}$ **:**

Given r_0, v_0 , and the propagation interval, $\Delta t = t - t_0$:

$$r_0 = \sqrt{x_o^2 + y_0^2 + z_0^2}\ , \tag{7.6}$$

$$h_0 = x_0\dot{x}_0 + y_0\dot{y}_0 + z_0\dot{z}_0\,, \tag{7.7}$$

$$v_0 = \sqrt{\dot{x}_0^2 + \dot{y}_0^2 + \dot{z}_0^2}\ , \tag{7.8}$$

$$\alpha = v_0^2 - \frac{2\mu}{r_0}\,, \tag{7.9}$$

$$\frac{1}{a} = -\frac{\alpha}{\mu}\,, \tag{7.10}$$

where a is the semi-axis major.

The eccentric anomaly and the eccentricity for the initial orbit are calculated by:

$$e\,sin\,E_0 = \frac{h_0}{\sqrt{\mu a}}\,, \tag{7.11}$$

$$e\,cos\,E_0 = 1 - \frac{r_0}{a}\text{, with } E_0 \text{ reduced to the interval 0 to } 2\pi. \tag{7.12}$$

The mean anomalies for the initial and propagated orbits, M_0 and M are given by:

$$M_0 = E_0 - e\,sin\,E_0\,, \tag{7.13}$$

$$n = \sqrt{\frac{\mu}{a^3}}\ , \tag{7.14}$$

$$M = n\Delta t + M_0\text{, with } M_0 \text{ and } M \text{ reduced to the interval 0 to } 2\pi. \tag{7.15}$$

The eccentric anomaly for the propagated orbit is calculated through the Kepler's equation. The variation of the eccentric anomaly is calculated and reduced to the interval 0 to 2π by:

$$\Delta E = E - E_0\,, \qquad\qquad 0 \le \Delta E \le 2\pi\ . \tag{7.16}$$

The transcendental functions s_0, s_1, s_2 for the elliptical orbit, according to Goodyear, are calculated by:

$$s_0 = cos\,\Delta E\,, \tag{7.17}$$

$$s_1 = \sqrt{\frac{a}{\mu}}\,sin\,\Delta E\,, \tag{7.18}$$

$$s_2 = \frac{a}{\mu}(1 - s_0). \tag{7.19}$$

Therefore, the functions f, g, $\dot{f}$, $\dot{g}$ are calculated by:

$$r = r_0 s_0 + h_0 s_1 + \mu s_2\,, \tag{7.20}$$

$$f = 1 - \frac{\mu s_2}{r_0}\,, \tag{7.21}$$

$$g = r_0 s_1 + h_0 s_2\,, \tag{7.22}$$

$$\dot{f} = -\frac{\mu s_1}{r r_0}\,, \tag{7.23}$$

$$\dot{g} = 1 - \frac{\mu s_2}{r}\,. \tag{7.24}$$

There is no singularity problem and the Kepler's equation is solved through the Newton Raphson's Method in double precision. The classical parameters a, e, i, Ω, ω, are constant in the Keplerian motion and, therefore, there is no different subscript for them.

The evaluation of the matrix M

First of all, it is necessary to calculate the secular component U including the effect of multi-revolution in the case of orbit propagation time, Δt, is bigger than one orbital period:

$$\Delta E = \Delta E + IFIX\left(\Delta t\,\frac{n}{2\pi}\right)2\pi\,, \tag{7.25}$$

$$s_4' = cos\,\Delta E - 1\,, \tag{7.26}$$

$$s_5' = \sin\Delta E - \Delta E\,, \tag{7.27}$$

$$U = s_2\Delta t + \sqrt{\left(\frac{a}{\mu}\right)^5}\left(\Delta E s_4' - 3s_5'\right), \tag{7.28}$$

where *IFIX(x)* provides the truncated integer number of the real argument *x*, and the variables s_4' and s_5' are related with the transcendental functions s_4 and s_5 (Goodyear, 1965, 1966).

Therefore, the components of the matrix *M* are given by :

$$M_{11} = \left(\frac{s_0}{rr_0} + \frac{1}{r_0^2} + \frac{1}{r^2}\right)\dot{f} - \mu^2\frac{U}{r^3 r_0^3}\,,$$

$$M_{12} = \left(\frac{\dot{f}s_1}{r} + \frac{(\dot{g}-1)}{r^2}\right),$$

$$M_{13} = \frac{(\dot{g}-1)s_1}{r} - \mu\frac{U}{r^3}\,,$$

$$M_{21} = -\left(\frac{\dot{f}s_1}{r_0} + \frac{(f-1)}{r_0^2}\right),$$

$$M_{22} = -\dot{f}s_2\,, \tag{7.29}$$

$$M_{23} = -(\dot{g}-1)s_2\,,$$

$$M_{31} = \frac{(f-1)s_1}{r_0} - \mu\frac{U}{r_0^3}\,,$$

$$M_{32} = (f-1)s_2\,,$$

$$M_{33} = gs_2 - U\,.$$

The property of the transition matrix

The inverse matrix $\boldsymbol{\Phi}^{-1}$, that propagates deviations from t to t_0, is given by:

$$\boldsymbol{\Phi}^{-1} = \begin{pmatrix} \boldsymbol{\Phi}_{22}^{T} & -\boldsymbol{\Phi}_{12}^{T} \\ -\boldsymbol{\Phi}_{21}^{T} & \boldsymbol{\Phi}_{11}^{T} \end{pmatrix}, \tag{7.30}$$

that results from the canonic nature of the original equations (Danby, 1964; Battin, 1964).

7.2 Second Method: The Markley Method

The state transition's differential equation is defined as:

$$\frac{d\boldsymbol{\Phi}(t,t_0)}{dt} = \begin{bmatrix} \boldsymbol{0} & \boldsymbol{I} \\ \boldsymbol{G(t)} & \boldsymbol{0} \end{bmatrix} \boldsymbol{\Phi}(t,t_0) \tag{7.31}$$

where $\boldsymbol{\Phi}(t_0,t_0) \equiv \boldsymbol{I}$ is the initial condition,

$$\boldsymbol{\Phi}(t,t_0) = \begin{bmatrix} \dfrac{\partial \boldsymbol{r}}{\partial \boldsymbol{r}_0} & \dfrac{\partial \boldsymbol{r}}{\partial \boldsymbol{v}_0} \\ \dfrac{\partial \boldsymbol{v}}{\partial \boldsymbol{r}_0} & \dfrac{\partial \boldsymbol{v}}{\partial \boldsymbol{v}_0} \end{bmatrix} \tag{7.32}$$

where $\boldsymbol{r} = (x \quad y \quad z)$ and $\boldsymbol{v} = (\dot{x} \quad \dot{y} \quad \dot{z})$ are the Cartesian state at the instant t, $\boldsymbol{r_0}$ and $\boldsymbol{v_0}$ are the Cartesian state in t_0 , $\boldsymbol{0}$ ≡ matrix 3x3 of zeros, $\boldsymbol{I}$ ≡ identity matrix 3x3, $\boldsymbol{G(t)}$ ≡ $\dfrac{\partial \boldsymbol{f}(\boldsymbol{r},t)}{\partial \boldsymbol{r}}$ ≡ gradient matrix, and $\boldsymbol{f}(\boldsymbol{r},t)$ = acceleration of the satellite.

Developing the Markley's method, the transition matrix for position and velocity is given by:

$$\boldsymbol{\Phi}(t,t_0) \approx \begin{bmatrix} \boldsymbol{\Phi}_{rr} & \boldsymbol{\Phi}_{rv} \\ \boldsymbol{\Phi}_{vr} & \boldsymbol{\Phi}_{vv} \end{bmatrix}_{6x6} \tag{7.33}$$

where

$$\boldsymbol{\Phi}_{rr} \equiv \boldsymbol{I} + (2\boldsymbol{G}_0 + \boldsymbol{G})\frac{(\Delta t)^2}{6},$$

$$\boldsymbol{\Phi}_{rv} \equiv \boldsymbol{I}\Delta t + (\boldsymbol{G}_0 + \boldsymbol{G})\frac{(\Delta t)^3}{12},$$

(7.34)

$$\boldsymbol{\Phi}_{vr} \equiv (\boldsymbol{G}_0 + \boldsymbol{G})\frac{(\Delta t)}{2},$$

$$\boldsymbol{\Phi}_{vv} \equiv \boldsymbol{I} + (\boldsymbol{G}_0 + 2\boldsymbol{G})\frac{(\Delta t)^2}{6}.$$

where $\Delta t \equiv t - t_0$ and $\boldsymbol{G}_0 \equiv \boldsymbol{G}(t_0)$.

The $\boldsymbol{G}$ and, therefore, $\boldsymbol{\Phi}_{rr}, \boldsymbol{\Phi}_{rv}, \boldsymbol{\Phi}_{vr}, \boldsymbol{\Phi}_{vv}$ are symmetric if the perturbation has a potential. The $\boldsymbol{G}$ gradient matrix including only the central force and the J_2 is given by:

$$\boldsymbol{G}(t_k) = \frac{\partial \boldsymbol{f}(\boldsymbol{r}, t_k)}{\partial \boldsymbol{r}} = \begin{bmatrix} \frac{\partial f_x}{\partial x} & \frac{\partial f_x}{\partial y} & \frac{\partial f_x}{\partial z} \\ \frac{\partial f_y}{\partial x} & \frac{\partial f_y}{\partial y} & \frac{\partial f_y}{\partial z} \\ \frac{\partial f_z}{\partial x} & \frac{\partial f_z}{\partial y} & \frac{\partial f_z}{\partial z} \end{bmatrix}. \tag{7.35}$$

The accelerations due to Earth's flattening are given by:

$$f_x = \frac{-\mu x}{r^3}\left[1 + \frac{3}{2}\frac{J_2 r_e^2}{r^2}\left(1 - \frac{5z^2}{r^2}\right)\right],$$

$$f_y = \frac{y}{x} f_x, \tag{7.36}$$

$$f_z = \frac{-\mu z}{r^3}\left[1 + \frac{3}{2}\frac{J_2 r_e^2}{r^2}\left(3 - \frac{5z^2}{r^2}\right)\right].$$

The partial derivatives are (Kuga, 1982):

$$\frac{\partial f_x}{\partial x} = \frac{\mu}{r^5}\left[3x^2 - r^2 - \frac{3}{2}J_2 r_e^2 + \frac{15}{2}\frac{J_2 r_e^2}{r^2}\left(x^2 + y^2\right) - \frac{105}{2}\frac{J_2 r_e^2}{r^4}x^2 z^2\right],$$

$$\frac{\partial f_x}{\partial y} = \frac{3\mu xy}{r^5}\left[1 + \frac{5}{2}\frac{J_2 r_e^2}{r^2} - \frac{35}{2}\frac{J_2 r_e^2}{r^4}z^2\right], \tag{7.37}$$

$$\frac{\partial f_x}{\partial z} = \frac{3\mu xz}{r^5}\left[1 + \frac{15}{2}\frac{J_2 r_e^2}{r^2} - \frac{35}{2}\frac{J_2 r_e^2}{r^4}z^2\right].$$

The transition matrix for clock bias, clock drift, and drift rate is given by:

$$\boldsymbol{\Phi}(t, t_0) = \begin{bmatrix} 1 & 0 & 0 \\ 0 & 1 & 0 \\ 0 & 0 & 1 \end{bmatrix}. \tag{7.38}$$

8. DATA SET

To validate and to analyze the algorithm, the data of the Topex/Poseidon (T/P) satellite is used. The following files are used:

- the T/P observation files that broadcast the code and carrier pseudoranges measurements in two frequencies in 10-second GPS time steps and are provided by GPS Data Processing Facility of the Jet Propulsion Laboratory in Rinex format (Shapiro, 1998);
- the T/P Precise Orbit Ephemeris (POE) files that are generated by the Jet Propulsion Laboratory (JPL) in one minute UTC time steps in the Inertial True of Date coordinates; and
- the broadcast GPS navigation message file in Rinex format provided by Crustal Dynamics Data Information System (CDDIS) of the Goddard Space Flight Center (Noll,. 1998).

The position and velocity estimated are compared against the T/P-POE. The T/P-POE is claimed to estimate T/P position to an accuracy better than 15 cm. The states in the POE are provided in one minute UTC time steps in Inertial True of Date coordinates. But, the T/P GPS measurements are provided in 10 seconds of GPS time. Accordingly to IERS, the difference between the UTC and GPS time is approximately an integer number of seconds, increasing timely with the introduction of leap seconds. For example, for 1993, the difference was 9 seconds. Therefore, it was necessary to interpolate the states through an interpolation (Polint) subroutine (Press *et. al.*, 1992). With this approach, the mean error of the interpolated states is 0.068 m and 2.5×10^{-4} m/s for position and velocity, respectively.

8.1 Topex/Poseidon satellite

This mission is jointly conducted by the United States National Aeronautics and Space Administration (NASA) and the French space agency, *Centre National d'Etudes Spatiales* (CNES). The main goal of this mission is to improve the knowledge of the global ocean circulation. Other applications include the ocean tides, geodesy and geodynamics, ocean wave height, and wind speed.

The T/P spacecraft orbits the Earth at an altitude of 1336 km, inclination of 66^o, and with nearly zero eccentricity. The period of the orbit is 1.87 hours.

This satellite carries a total of five tracking systems including Satellite Laser Ranging (SLR), DORIS Doppler, GPS, TDRSS, and the satellite altimeter itself. The satellite orbit must be determined with a RMS radial accuracy of 13 centimeters. This is an extremely stringent accuracy requirement for a satellite of this shape and altitude. T/P carries a dual frequency receiver GPS onboard experimentally to test the ability of the GPS to provide precise orbit determination (POD). This receiver can track up to 6 GPS satellites at once on both frequencies if Anti-Spoofing is inactive.

9. GPS EPHEMERIDES

There are three sets of data available to determine position and velocity vectors of the GPS satellites in a terrestrial reference frame at any instant. They are the almanac data, the broadcast ephemeris, and the precise ephemerides

The almanac data contain parameters for the orbit and satellite clock correction terms for all satellites and they are updated at least every six days. They provide the user with less precise data to facilitate receiver satellite search or for planning task such as the computation of visibility charts. They are broadcast as part of the satellite message.

The broadcast ephemerides contains general, orbital and satellite clock information. They are based on observations at the five stations of the GPS control segment. The most recent of these data are used to compute a reference orbit for the satellites. They are broadcast as part of the satellite message, updated every hour and converted to Rinex format. They should only be used during the prescribed period of approximately four hours to which they refer. The algorithm to calculate the position and velocity vectors can be found in Leick (1997).

The precise ephemerides consist of satellite positions and velocities in 15-minute interval in SP3 format. They are produced by the Naval Surface Warfare Center (NSWC) together with the Defense Mapping Agency (DMA) and are based on observed data in the tracking network of the control segment. The most accurate orbital information is provided by the IGS with a delay of about two weeks.

The uncertainty of ephemerides provided by the almanac data is of some kilometers and depends on the age of the data. For broadcast with SA on, it is of 5 –100 m and depending on the level of SA. For broadcast with SA off, it is of 5-10 m or even better. For precise ephemeris, it is of order of 0.2 – 2m or even better (Hofmann-Wellenhof *et. al.*, 1994).

9.1 Broadcast Ephemerides Analyses

The algorithm shown in Leick (1997) has been implemented, in Fortran language, by H. Kuga at INPE to determine the position of GPS satellites using the broadcast ephemerides. This software is used in this OBODE-GPS. The main goal of this analyses is to check to which extent the GPS position error can affect the estimated orbit.

To analyze the GPS position error generated by the broadcast ephemeris, a comparison has been done with precise orbit ephemerides POE generated by JPL. Figures 9.1 to 9.7 show the error among them for each satellite for one day. Tables 9.1 to 9.7 show the comparative statistics between the GPS position calculated using the broadcast and precise ephemerides, respectively, for the same day.

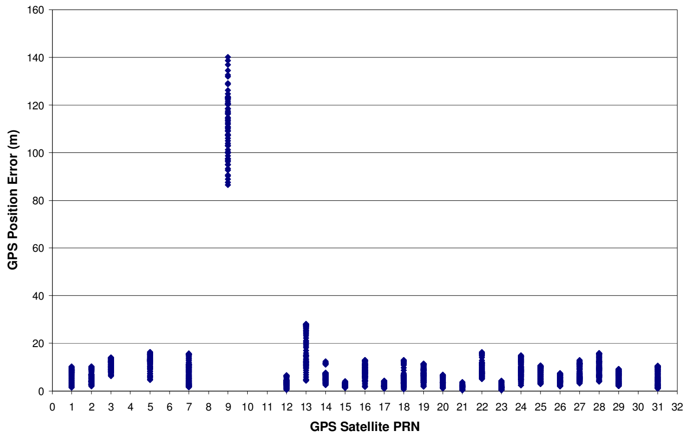

Figure 9.1: GPS position error for 1993/11/18

Table 9.1: Statistical error of the GPS position for 1993/11/18

Mean error	9.56 m
Standard Deviation error	17.94 m
Maximum error	140.05 m
Minimum error	0.34 m

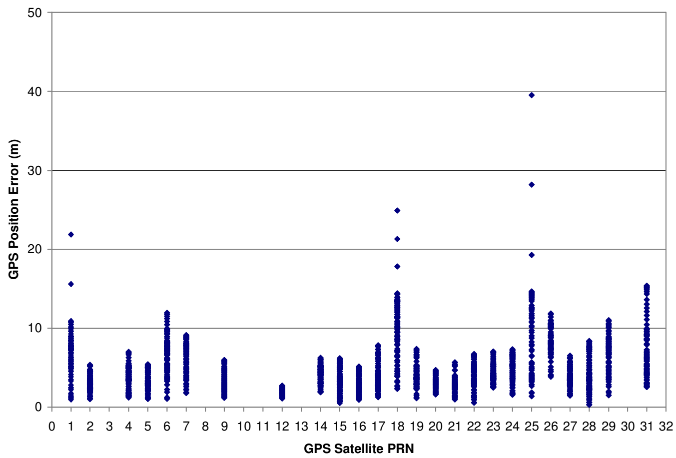

Figure 9.2: GPS position error for 1995/04/25

Table 9.2: Statistical error of the GPS position for 1995/04/25

Mean error	4.89 m
Standard Deviation error	2.99 m
Maximum error	39.53 m
Minimum error	0.29 m

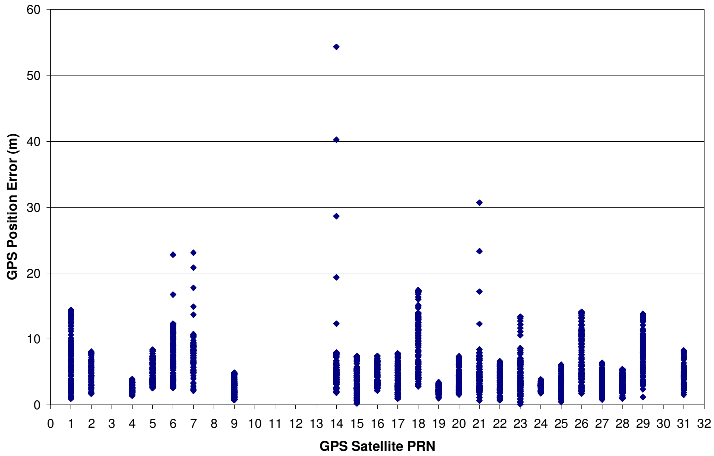

Figure 9.3: GPS position error for 1996/03/14

Table 9.3: Statistical error of the GPS position for 1996/03/14

Mean error	4.91 m
Standard Deviation error	3.46 m
Maximum error	54.31 m
Minimum error	0.14 m

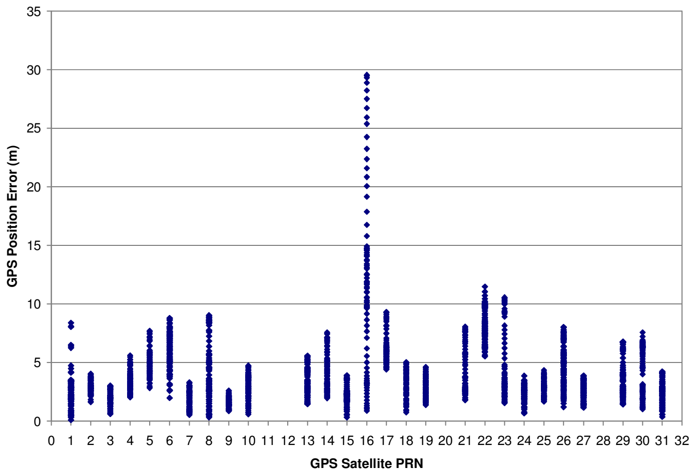

Figure 9.4: GPS position error for 1998/01/07

Table 9.4: Statistical error of the GPS position for 1998/01/07

Mean error	3.94 m
Standard Deviation error	2.91 m
Maximum error	29.55 m
Minimum error	0.08 m

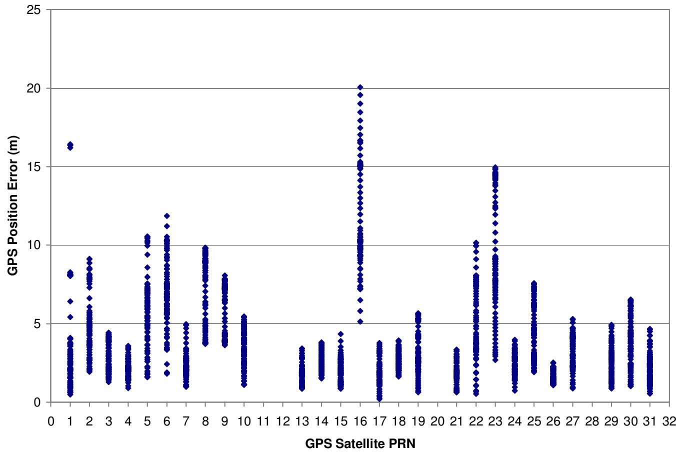

Figure 9.5: GPS position error for 1998/06/08

Table 9.5: Statistical error of the GPS position for 1998/06/08

Mean error	4.01 m
Standard Deviation error	2.96 m
Maximum error	20.05 m
Minimum error	0.2 m

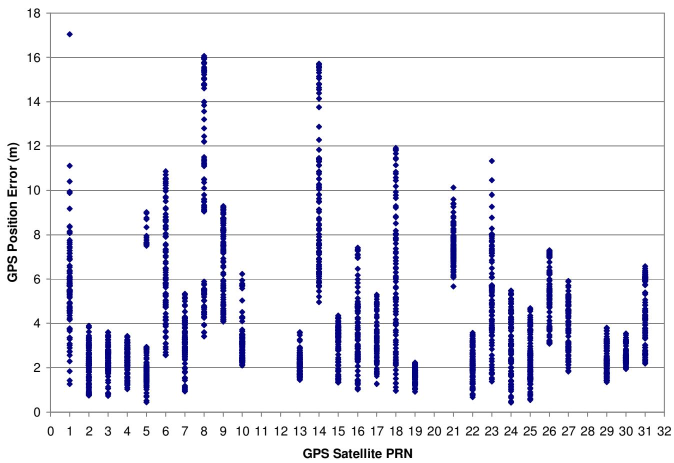

Figure 9.6: GPS position error for 1999/01/24

Table 9.6: Statistical error of the GPS position for 1999/01/24

Mean error	4.19 m
Standard Deviation error	2.79 m
Maximum error	17.08 m
Minimum error	0.44 m

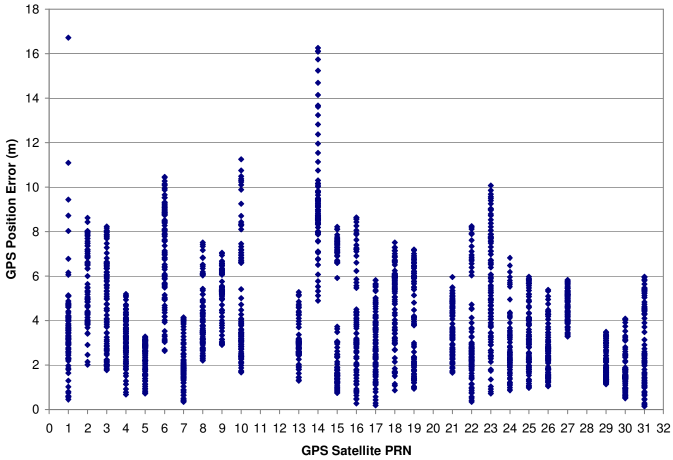

Figure 9.7: GPS position error for 1999/12/16

Table 9.7: Statistical error of the GPS position for 1999/12/16

Mean error	3.97 m
Standard Deviation error	2.35 m
Maximum error	16.72 m
Minimum error	0.13 m

In November, 18th, 1993, the satellite PRN 9 did not provide good data. The other days, the maximum error was around 40m during some intervals, which is reasonable and do not affect the estimation of the satellite. These results show that the software is reliable and it can be used to calculate the GPS position using the broadcast message.

10.TESTS

Some tests related to the dynamical model and to the estimation technique have been performed. The goal is to have low computational cost with relative accuracy around tens of meters. The first test has been done with respect to the gravitational model. The 50th order and degree of the spherical harmonic coefficients of the JGM-2 model has been used in Chiaradia *et al*. (1999), a previous work. The second test has been done with respect to the step size of the RK4 integrator. The T/P observation file broadcast measurement in 10 second interval. In Chiaradia *et al*. (1999), the step size used was 10 seconds in the same epoch of the observation file.

10.1 First Test: Gravitational Model

All tests have been done for the whole day 1993, November, 18th. The order and degree of the spherical coefficients of the JGM-2 has been changed and the filter was off. Each case was compared with T/P precise orbit ephemerides (POE). The Table 10.1 shows the parameters of the Kalman filter.

Table 10.1: Parameter of the Kalman filter

Measurement standard deviation σ_{xyz} (m)	100
A priori std. dev. position σ_{pos} (m)	1000
A priori std. dev. velocity σ_{vel} (m/s)	10
A priori std. dev. bias σ_{bias} (m)	1000
A priori std. dev. drift σ_{drift} (m/s)	10
A priori std. dev. drift rate σ_{rates} (m/s^2)	1.0×10^{-8}
State noise position w_{pos} (m)	0.5
State noise velocity w_{vel} (m/s)	0.0005
State noise bias w_{bias} (m)	0.5
State noise drift w_{drift} (m/s)	0.0005
State noise drift rate w_{rate} (m/s^2)	1.0×10^{-10}

Table 10.2 shows the comparison between each gravitational model and T/P POE in different hours along the day. All results are meters.

Table 10.2: Comparison of the gravitational model

Time (h)	J_2	4x4	10x10	15x15	20x20	25x25	50x50
1.0	82	109	11	3.5	2.45	2.26	2.1
2.0	553	212	19	8	6.7	6.3	6.15
6.0	2673	490	30	16	11	13.45	12.8
12.0	2409	1028	30	32	28	31	30.3
18.0	3837	1493	34	46	37	41	42
24.0	4282	2217	97	32	19	33	36
Mean error	2572	1012	38	29	24	28	28
σ error	1251	590	23	15	14.2	17	17

The best results are obtained using the model up to 10^{th} order and degree which have a good accuracy and not too high computational cost. The more complete models, as 15^{th} to 50^{th}, have little improvement against high computational cost.

10.2 Second Test: Step Size of Propagation

All tests have been done for the whole day 1993, November, 18^{th}. The order and degree of the spherical coefficients of the JGM-2 is fixed in 10x10. Each case was compared with T/P precise orbit ephemerides (POE). Figures 10.1 to 10.8 show the position and velocity error and the respective standard deviation for each step size. Table 10.3 shows the mean and standard deviation error and RMS for position, velocity, and residuals in each step size. The following step sizes were tested: 10s, 30s, 60s, and 90s.

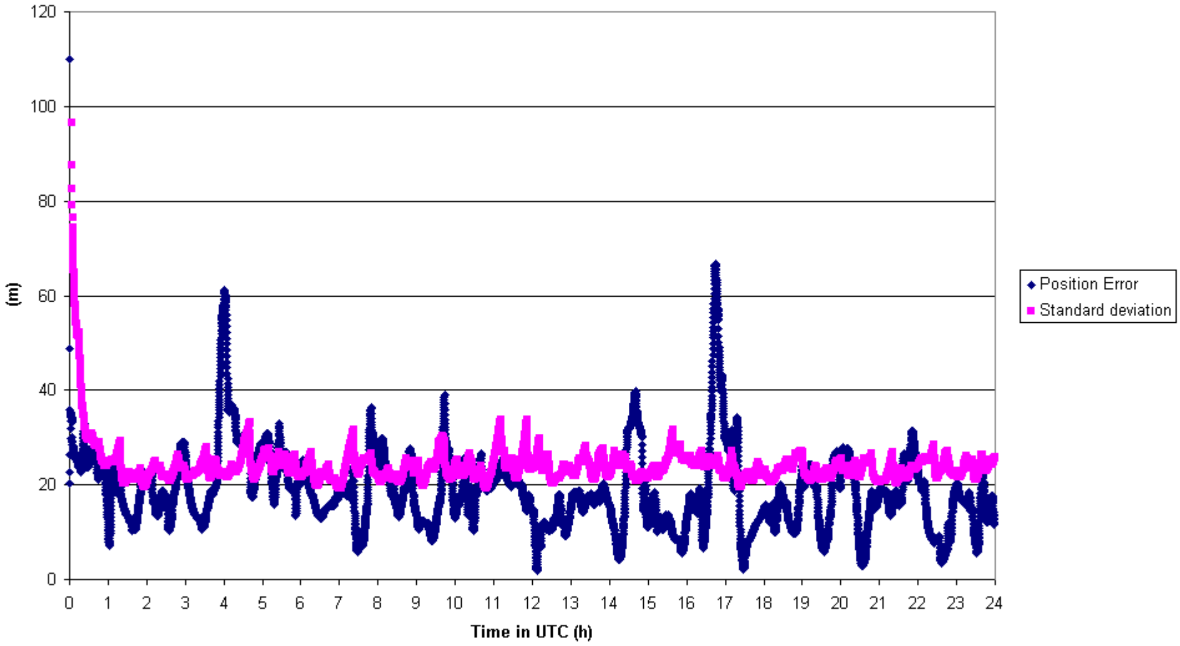

Figure 10.1: Position Error and Standard deviation for 10 s step size

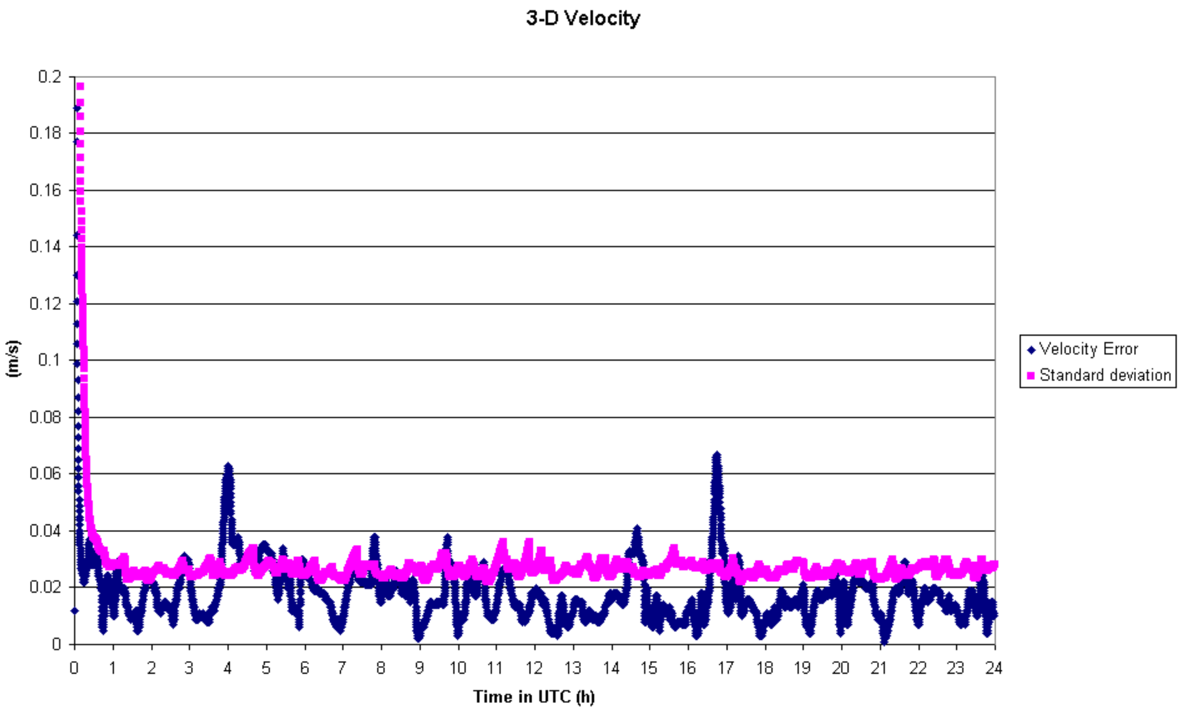

Figure 10.2: Velocity Error and Standard deviation for 10 s step size

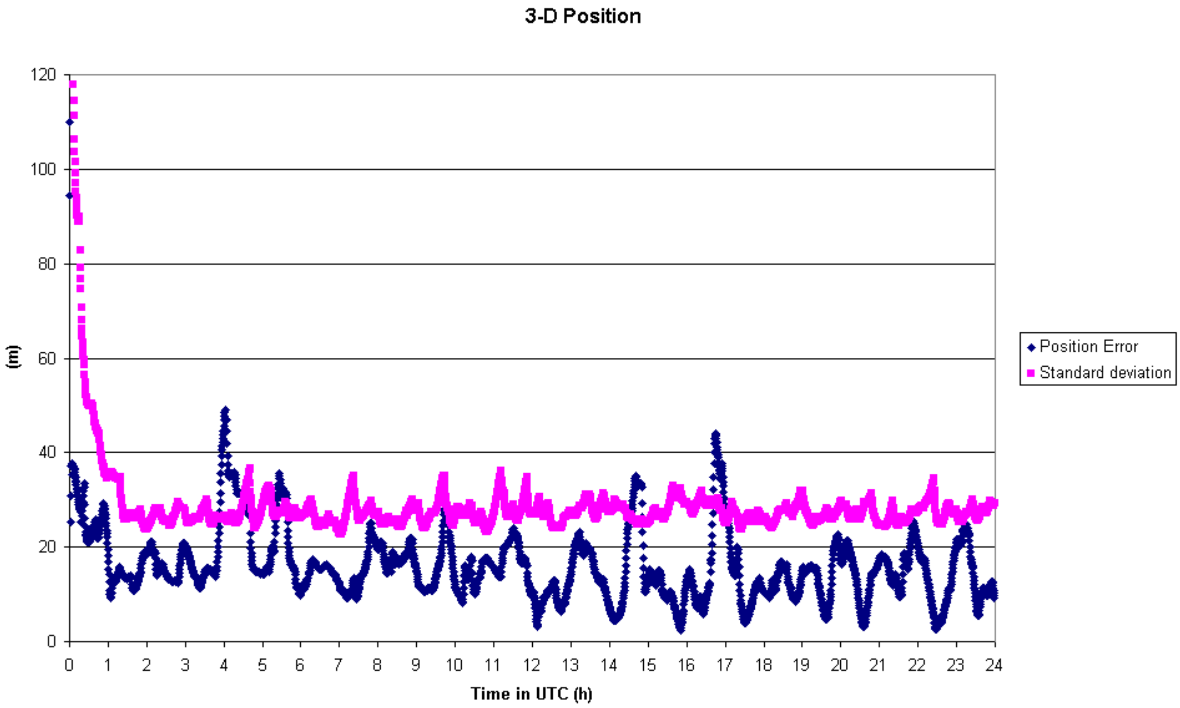

Figure 10.3: Position Error and Standard deviation for 30 s step size

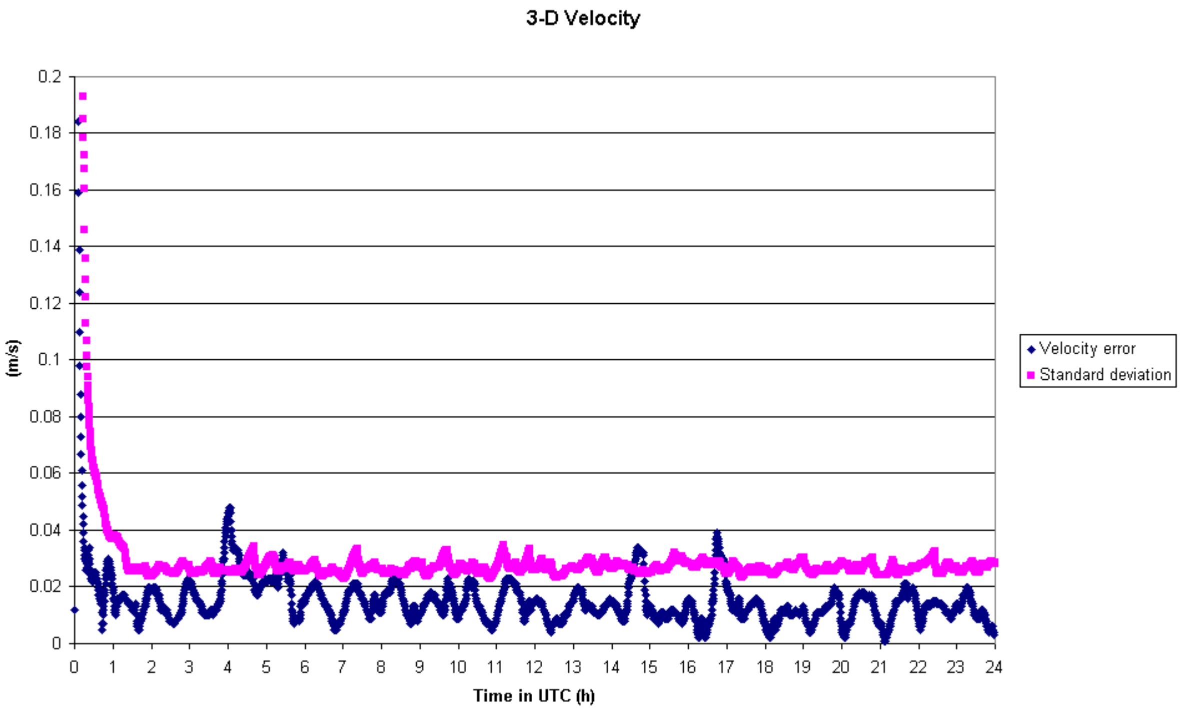

Figure 10.4: Velocity Error and Standard deviation for 30 s step size

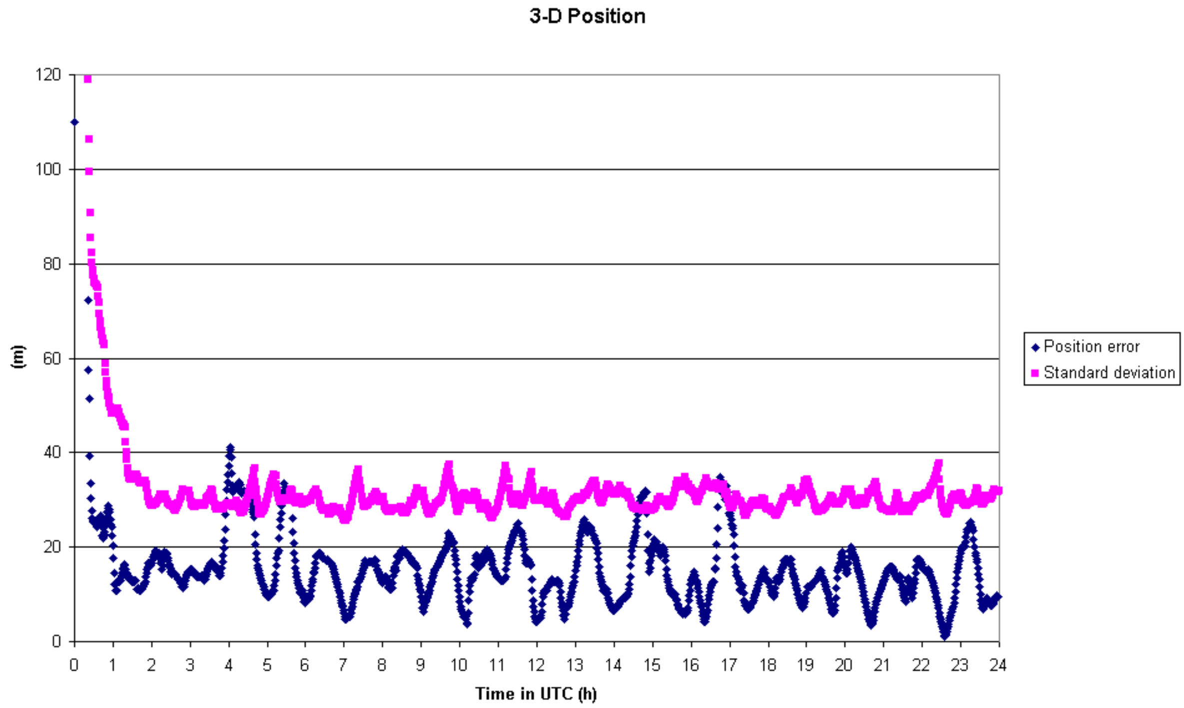

Figure 10.5: Position Error and Standard deviation for 60 s step size

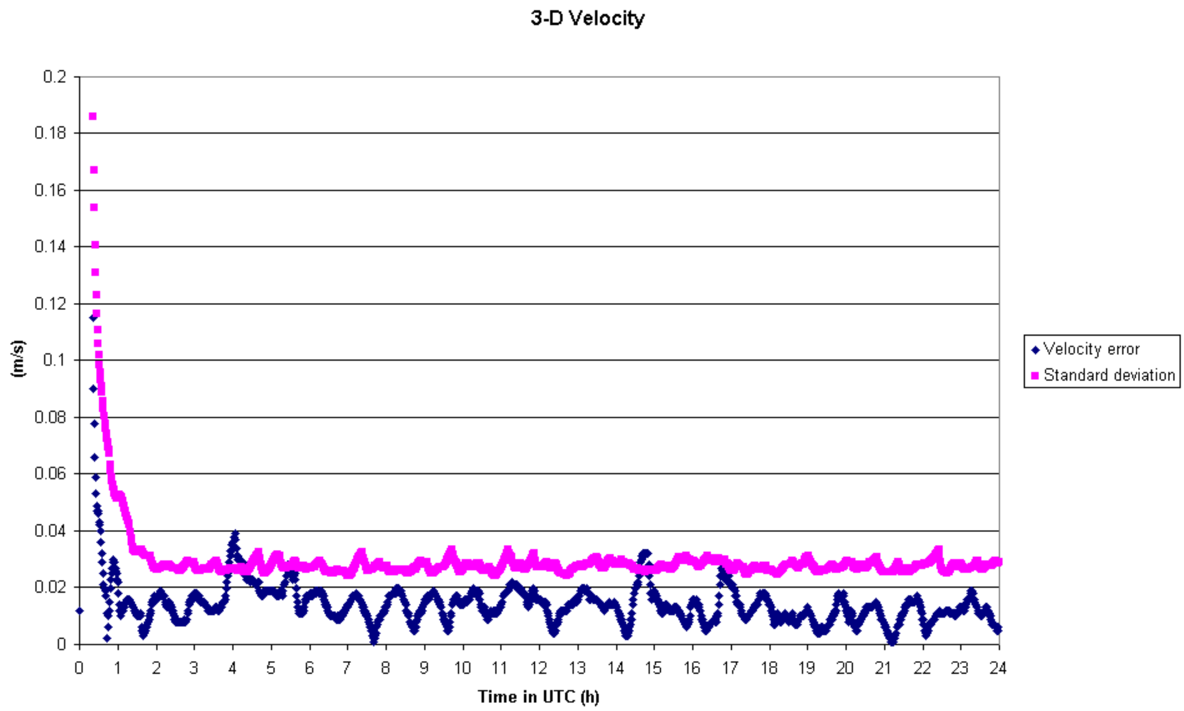

Figure 10.6: Velocity Error and Standard deviation for 60 s step size

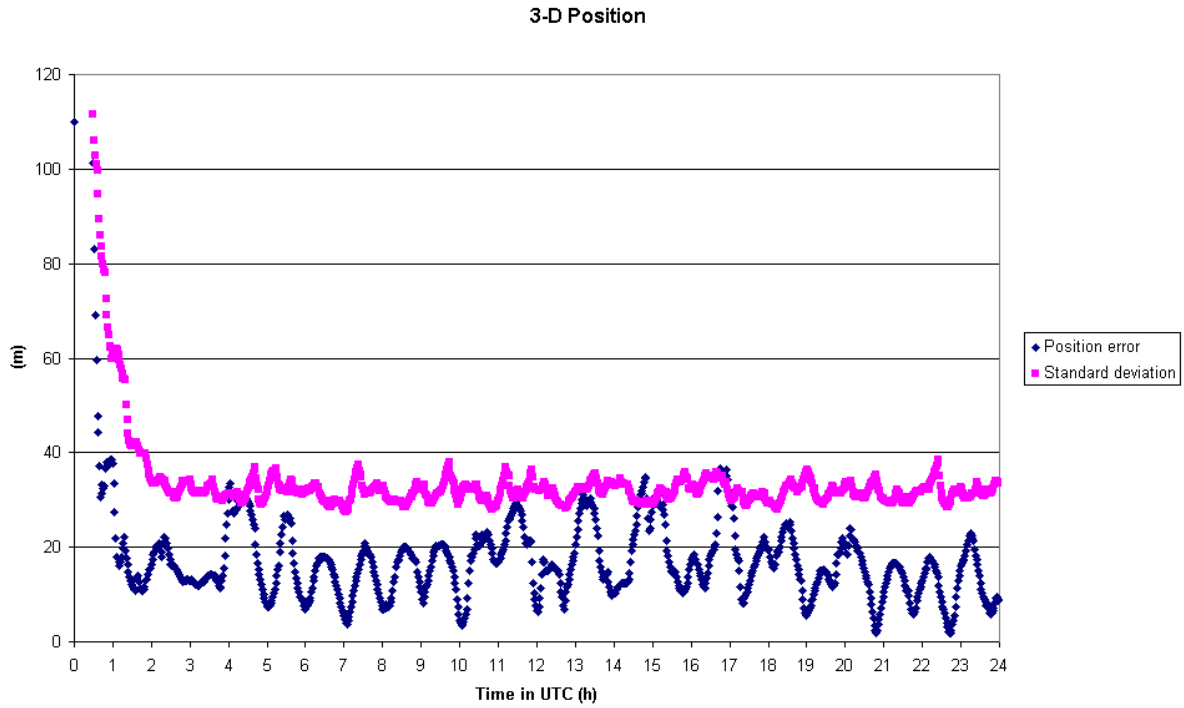

Figure 10.7: Position Error and Standard deviation for 90 s step size

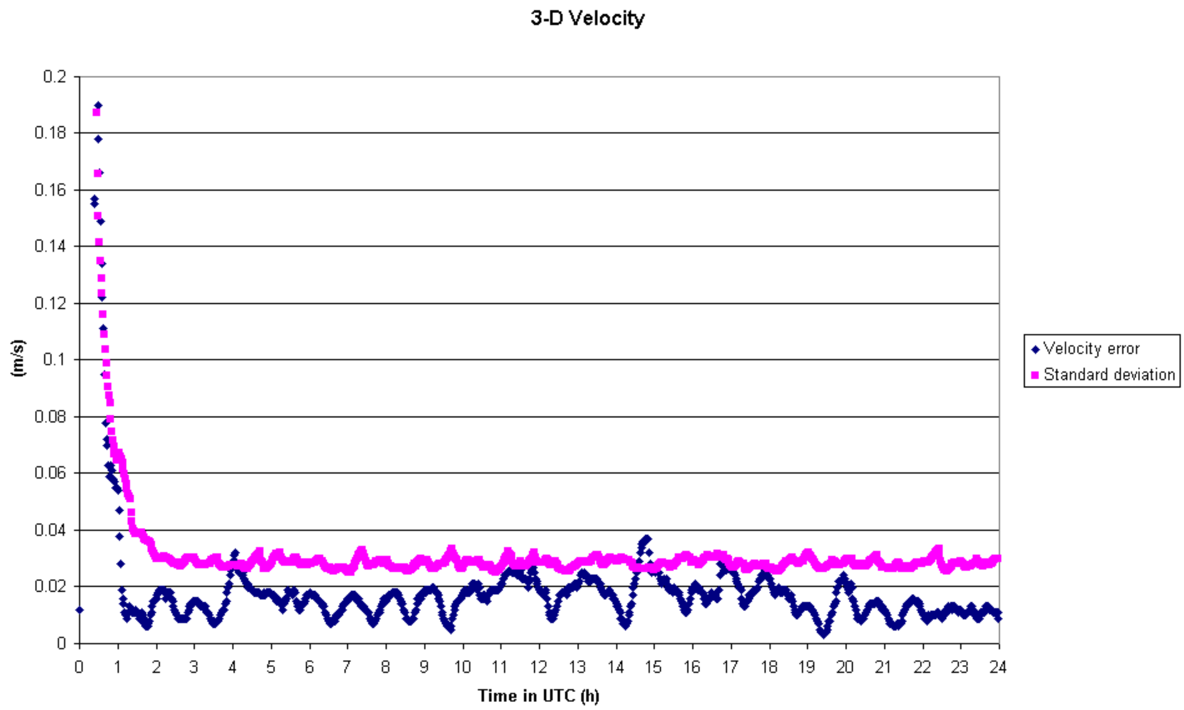

Figure 10.8: Velocity Error and Standard deviation for 90 s step size

Table 10.3: Comparison among the step sizes of the propagation

	Δt = 10s	**Δt = 30s**	**Δt = 60s**	**Δt = 90s**
Position RMS	20.62 m	18.02 m	96.37 m	110 m
Velocity RMS	0.072 m/s	0.1 m/s	0.31 m/s	0.25 m/s
Residuals mean error	0.195 m	0.25 m	0.168 m	42.17 m
Residuals σ error	12.02 m	12.02 m	15.94 m	5.27 m

The best results are obtained using 30 second step-size of propagation. In 10-second step size, all observations are used and it is possible that some bad data are present. In the first two cases, the estimated vector took less than one hour to converge and in the other cases, more than one hour.

10.3 Third Test: Transition Matrix

Two tests were done with respect to the transition matrix. In the first test, the Keplerian motion was implemented and, in the second one, the J_2 was implemented according to Chapter 7. In both tests, the 30-second step-size of propagation and 10^{th} order and degree of spherical harmonics coefficients were considered. Table 10.4 shows comparison between the two tests.

Table 10.4: Comparison between the models for the transition matrix

	Keplerian Motion	**J_2**
Position mean error	16.14 m	16.13 m
Position σ error	8.03 m	8.02 m
Velocity mean error	0.019 m/s	0.019 m/s
Velocity σ error	0.095 m/s	0.09 m/s
Residuals mean error	0.196 m	0.23 m
Residuals σ error	12.02 m	13.63 m

In accordance with Chiaradia *et. al*. (1999), the transition matrix considering the J_2 effect did not provide good results for whole day.

Figure 10.9 shows the residuals for the best case which the step size of propagation is 30 seconds and the gravitational model is up to 10^{th} order and degree.

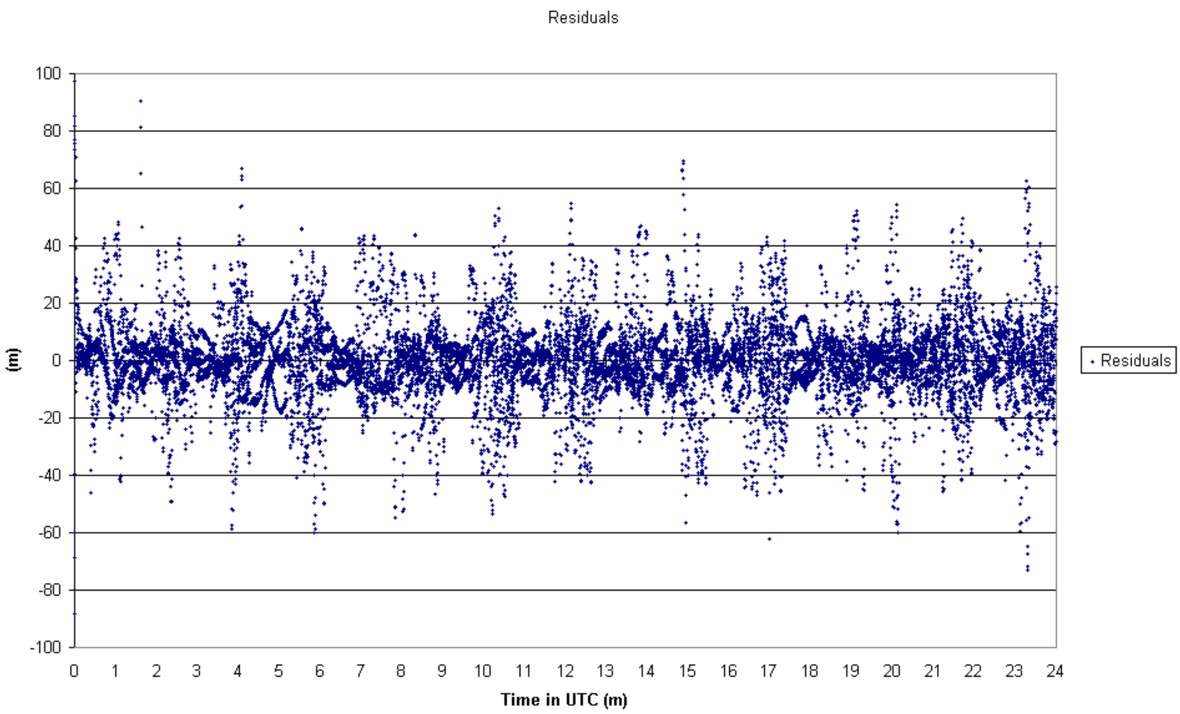

Figure 10.9: Residuals for the best case

11. CONCLUSIONS

The main goal of this work was to achieve accuracy around tens of meters along with minimum computational cost when determining in real time the artificial satellite orbits onboard considering a simplified model. To develop it, the single frequency GPS measurements are used, considering the effects of the clock offsets of the GPS and user satellites and user relativistic effects.

With respect to the dynamical model, the best results are obtained using the geopotential model up to 10th order and degree which provides a good accuracy at not high computational cost. The more complete models, as 15th to 50th order, presented a little improvement against high computational cost.

With respect to the step size of propagation, the best results are obtained using 30-second step-size of propagation. In 10-second step-size, all observations are used and it is possible that some local bad data are present. It is noted that the estimated state vector takes around one hour to converge in all cases.

With respect to the measurement model, it is not necessary to consider the ionospheric effect when the requirement of the mission is accuracy around tens of meters.

With respect to the transition matrix, the same results have been achieved using both methods, Keplerian and J_2 included. However, in the first case, which considers the pure Keplerian motion, the method was optimized to elliptical orbits (not dealing with parabolic or hyperbolic ones). In the second case (Markley's method), the expressions and the calculations are simpler than the first case. But, both cases require short propagation time for fair accuracy.

The GPS ephemeris generated through the broadcast message is calculated with good accuracy (less than 10 m) without affecting the estimated orbit accuracy. Some GPS satellites sometimes present a large error but, in principle, it does not affect the performance of the estimation procedure. These results show that the software is reliable and it can be used to calculate the GPS position using the broadcast message.

Summarizing, the satellite orbit has been estimated using the OBODE-GPS with a good accuracy and minimum computational cost: less than 20 m accuracy, using the 30 seconds step-size of propagation (10 second step-size can be used as well), the geopotential model up to 10th order and degree, and the propagation method of the transition matrix considering the J_2 effects.

12.REFERENCES

Battin, R. H.; *Atronautical Guidance*. New York, Academic, 1964.

Chiaradia A. P. M., Kuga H. K., Prado A. F. B. A.; Investigation of simplified models for orbit determination using single frequency GPS measurements. Presented in 14th *International Symposium on Space Flight Dynamics*, Foz de Iguaçu, Brazil, 1999, RBCM, J. of the Braz. Soc. Mechanical Sciences, Vol. XXI – Special Issue – 1999, pp. 165-172.

Danby J. M. A.; The matrizant of Keplerian motion. *AIAA Journal*, 2(1): 16-19, Jan.,1964.

Gelb A., Kasper Jr. J.F., Nash Jr. R.A., Price C.F.; Sutherland Jr., A.A.; *Applied Optimal Estimation*. The M.I.T. Press, England, 1974. 374p.

Goodyear W. H.; Completely general closed-form solution for coordinates and partial derivatives of the two-body problem. *The Astronomical Journal*, 70(3): 189-192, Apr., 1965.

Goodyear W. H.; A general method for the computation of Cartesian coordinates and partial derivatives of the two-body problem. Greenbelt, MD, *Goddard Space Flight Center* (NASA CR-522), Sept, 1966.

Hofmann-Wellenhof B., Lichtenegger H., Collins J.; *Global Positioning System – Theory and Practice*. Springer-Verlag Wien New York, 1994. 355p.

Kondapalli R. R.; A review on numerical methods for initial value problems. (INPE- 3011-RPI/088), INPE, Brazil, 1984.

Kuga H. K.; Estimação adaptativa de órbitas aplicada a satélites a baixa altitude. *Master Thesis* (INPE-2316-TDL/079), INPE, Brazil,1982. (in Portuguese).

Kuga H. K.; *Matriz de Transição do Movimento Kepleriano Elíptico*,. (INPE-3779-NTE/250), INPE, Brazil, 1986. (in Portuguese).

Kuga H. K.; Determinação de órbitas de satélites artificiais terrestres através de técnicas de estimação combinadas a técnicas de suavização de estado. *Ph.D. Dissertation* (INPE-4959-TDL/079), INPE, Brazil, 1989. (in Portuguese).

Kuga H. K.; Gill E.; *A Mathematical Description of the ODEM Orbit Determination Software*. DLR-GSOC-IB-94-06, DLR, Germany,1994.

Kuga H. K.; Gill E.; Montenbruck O.; *Orbit Determination and Apogee Boost Maneuver Estimation Using UD-filtering*. DLR-GSOC IB 91-2, DLR, Germany,1991.

Leick A.; *GPS Satellite Surveying*. 2nd edition. John Wiley & Sons, INC., 1995. 560p.

Markley F. L.; Approximate Cartesian State Transition Matrix. *The Journal of the Astronautical Sciences.* Vol. 34, n. 2, p161-169, apr-jun, 1986.

Maybeck P. S.; *Stochastic Models, Estimation, and Control*. Vol. 1, Academic Press, London, 1979. 423p.

Montenbruck O., Gill. E.; *Satellite Orbits – Models, Methods, and Applications.* Springer Verlag, Heidelberg, 2000.

Noll C.; *Crustal Dynamics Data Information System.* [On-line] ftp://cddisa.gsfc.nasa.gov/, Dec., 1998.

Press H. W., Flannery B. P., Teukolsky S. A., Vetterling W. T.; *Numerical Recipes*. Cambridge University Press, 3rd edition, 1987. 818p.

Pines S.; Uniform representation of the gravitational potential and its derivatives. *AIAA Journal*, Vol.11, No.11, Nov., 1973.

Shapiro B. R.; *Topex/ Poseidon Navigation Team.* [On-line] http://topexnav.jpl.nasa.gov., April, 1998.

Shepperd S. W.; Universal Keplerian state transition matrix. *Celestial Mechanics,* 35: 129-144, 1985.

Tapley B. D., Ries J. C., Davis G. W., Eanes R.,J., Schutz B.E., Shum C.,K., Watkins M.,M., Marshall J.,A., Nerem R. S., Putney B. H., Klosko S. M., Luthcke S. B.; Pavlis D., Williamson R. G., Zelensky N. P.; Precision orbit determination for TOPEX/Poseidon. *Journal of Geophysical Research*, Vol. 99, n. C12, p24383-24404, dezembro, 1994.